Ni/SiO_2 Materials Prepared by Deposition−Precipitation: Influence of the Reduction Conditions and Mechanism of Formation of Metal Particles

Paolo Burattin,[†] Michel Che,[‡] and Catherine Louis*

Laboratoire de Réactivité de Surface, UMR 7609 CNRS,Université Pierre et Marie Curie, 4 place Jussieu, 75252 Paris Cedex 05, France

Received: January 27, 2000; In Final Form: July 19, 2000

The influence of the parameters of temperature-programmed reduction (TPR) on the size of the metal particles and on the extent of nickel reduction was investigated for a Ni/SiO_2 sample (24 wt % Ni) prepared by deposition−precipitation whose supported phase is a 1:1 nickel phyllosilicate. Three reduction parameters were investigated: the gas flow rate, the heating rate, and the final reduction temperature. The size of the metal particles and the extent of nickel reduction were determined by transmission electron microscopy, hydrogen chemisorption, chemical titration by sulfuric acid, and magnetic measurements. The results show that TPR up to 900 °C leads to fully reduced nickel particles whose average size varies between 35 and 65 Å, depending on the reduction parameters. It has been possible to get smaller particles of about 20 Å by isothermal reduction at 450 °C, but nickel was not fully reduced. Experiments on the sintering of the nickel oxide particles before reduction and of the nickel metal particles showed that it was not possible to obtain metal particles larger than 70 Å, probably owing to a strong metal oxide− and metal−support interaction, respectively. A mechanism of formation of metal particles for samples prepared by deposition−precipitation is proposed.

Introduction

This paper is the last contribution of a study devoted to the preparation and characterization of Ni/SiO_2 catalysts prepared by deposition−precipitation (DP).[1−3]

The first paper was devoted to the characterization of the supported Ni(II) phase.[1] The nature of the latter was shown to depend on several parameters such as the characteristics of silica (surface area and morphology) and the DP time. For short DP times ($\leq$4 h) and with silicas of low surface area, the Ni(II) phase is mainly a turbostratic nickel hydroxide,[4] while with silicas of high surface area, it is mainly an ill-crystallized 1:1 nickel phyllosilicate[5] (Figure 1). For long DP times ($>$4 h) and with both types of silica, the Ni(II) phase is a 1:1 nickel phyllosilicate.

In the second paper, a molecular mechanism was proposed in order to explain the chemical phenomena occurring during preparation.[2] The mechanism is based on a kinetic competition between two types of reactions: (i) Ni−O−Si heterocondensation/polymerization, which leads to the formation and growth of 1:1 nickel phyllosilicate on silica; (ii) Ni−OH−Ni olation/polymerization, which leads to the formation and growth of nickel hydroxide on silica.

The third paper dealt with the influence of the parameters of the preparation on the size of the metal particles obtained. Several sets of DP Ni/SiO_2 samples were reduced by temperature-programmed reduction (TPR)[3]. The results showed that the average size could vary between $\approx$25 and $\approx$80 Å, depending on the nature and reducibility of the supported Ni(II) phase, and on the extent of the interface between this phase and silica.

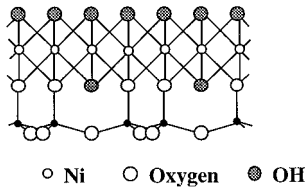

Figure 1. Structure of a layer of 1:1 nickel phyllosilicate (projection on the *bc* plane), from refs 16 and 17.

If the reducibility and the particle size of DP Ni/SiO_2 samples have been already discussed in the literature,[6−15] they have not been investigated systematically. The present paper deals with the influence of the reduction conditions on the metal particle size; the results lead to a discussion on the resistance of nickel particles to sintering, and the paper concludes with a mechanism on the formation of metal particles.

A DP Ni/SiO_2 sample with a high nickel loading (24 wt %) was chosen since it is expected to lead to a great variety of particle sizes. After preparation, the sample consists of a 1:1 nickel phyllosilicate phase supported on a porous silica of high surface area ($\approx$400 $m^2 \cdot g^{-1}$), which involves about 50 wt % of the original silica support.[1]

The reduction was performed either by TPR up to 800−900 °C or up to 450 °C and maintained at this temperature for various times. In the first case, three reduction parameters were studied: the flow rate of the reduction gas, the heating rate, and the final reduction temperature, with the aim at varying the average size of metal particles within a range as broad as possible and reaching a reduction as complete as possible.

Experimental Section

1. Sample Preparation. The Ni/SiO_2 sample was prepared by deposition−precipitation as described earlier.[1−3] It consists

* Corresponding author. E-mail: louisc@ccr.jussieu.fr.
[†] Institut Universitaire de France.
[‡] Permanent address: Rhône Poulenc CRIT-Carrières, 86 avenue des Frères Perret, BP 62, 69192 Saint Fons Cedex, France.

10.1021/jp0003151 CCC: $19.00
Published on Web 10/21/2000

of the precipitation of a nickel(II) phase onto silica support by basification of a nickel salt solution containing silica in suspension through decomposition of urea. Silica (3.8 g) was put into a vessel thermostated at 90 °C. An aqueous solution (500 mL) containing nickel nitrate (0.14 M), urea (0.42 M), and nitric acid (0.02 M) was added at $t = 0$ while the suspension (7.6 g·L^{-1} of silica) was magnetically stirred. The solution reached 90 °C within 3 min during which DP started and the pH changed according to ref 2. After 4 h of DP, the suspension was cooled to 20−25 °C and then filtered. The sample was washed three times as follows: after addition of 800 mL of distilled water, the resulting mixture was stirred for 10 min at 50−60 °C before filtration. Finally, the sample was dried in air at 90 °C for 24 h.

The silica support was a porous silica Spherosil XOA400 (Rhône-Poulenc, France, purity >99.5%, $S_{BET} = 356$ m^2·g^{-1}, pore volume = 1.25 cm^3·g^{-1}, average pore diameter = 80 Å). Nickel nitrate ($Ni(NO_3)_2$·$6H_2O$) was purchased from Aldrich (purity >99.0%).

The chemical analysis performed by inductive coupling plasma at the CNRS Center of Chemical Analysis (Vernaison, France) gave a Ni weight loading of 24 wt %.

2. Reduction Conditions. The TPR conditions were the same as those described earlier:[1−3] heating from room temperature to 900 °C with a rate of 7.5 °C·min^{-1}, under 5% v/v H_2 in Ar with a flow rate of 25 mL·min^{-1}. The only difference is that 200 mg of sample was used instead of 20 mg for the needs of characterization by other techniques (see below). Such conditions are considered to be the standard ones in the present paper.

In some cases, the Ni/SiO_2 sample was reduced in the following conditions:

a. By TPR from room temperature to 800 or 900 °C under a stream of 5% v/v H_2 in Ar with various heating rates (1−15 °C·min^{-1}) and various flow rates (10−100 mL·min^{-1}), respectively. These conditions of TPR were not optimal to study the TPR peak shapes since the parameter P defined by Mallet and Cabarello[18] varies between 15 and 275 K. According to these authors, P must be lower than 20 K to avoid distortion in the TPR profiles. So, only the TPR peak shifts are discussed in the present paper.

b. At 450 °C; the standard TPR procedure was followed up to 450 °C, and then the temperature was maintained at 450 °C for various durations. In this case, the reduction of nickel was incomplete. This latter procedure is hereafter referred to as isothermal reduction at 450 °C.

The extent of nickel reduction is deduced from the quantitative determination of the H_2 consumed during TPR. The calibration was performed by simulating total H_2 consumption: the H_2/Ar mixture flowing through the measurement arm of the catharometer detector was switched to pure Ar. The catharometer signal induced by this switch, which corresponds to 100% H_2 consumption, was integrated.

3. Techniques. The reduced samples were examined by transmission electron microscopy (TEM) with a JEOL JEM 100CXII electron microscope equipped with a top-entry device and operating at 100 kV. The histograms of metal particle sizes were established from the measurement of about 300 particles. The average particle diameter d was calculated from the following formula: $d = \sum n_i d_i / \sum n_i$, where n_i is the number of particles of diameter d_i. The detection limit is about 10 Å for nickel metal particles supported on silica.

The average particle size was also determined by hydrogen chemisorption. After reduction, the samples were cooled from the selected reduction temperature to 450 °C and purged under argon (25 mL·min^{-1}) at the same temperature for 1 h, so as to eliminate chemisorbed hydrogen. The so-called "monopoint" chemisorption method, proposed by Coenen[8,19] for the study of the same type of catalysts, was used under the following conditions: adsorption of ≈760 Torr of pure H_2 for 24 h at 27.4 °C. The amount of hydrogen chemisorbed was converted into an average Ni^0 particle size, assuming spherical particles and 5.71 Å^2 for the average surface area of one Ni atom (calculated from the thermodynamically stable structure of a Ni^0 particle, assumed to be composed of (111) plane (70%), (110) plane (5%), and (100) plane (25%)[20]).

TABLE 1: Extent of Nickel Reduction and Average Metal Particle Diameter in DP Ni/SiO_2 (24 wt % Ni) Reduced in Isotherm at 450 °C or by TPR Up to 900 °C under Standard Conditions. Comparison of the Results Obtained by Different Techniques

reduction conditions		extent of reduction (%)			av metal particle dia (Å)		
temp (°C)	time (h)	TPR	chemical titration	MM	TEM	H_2 chemisorpn	MM
450	5	36.4	36.3		21	19	
450	10	52.3, 52.6			21	22	25
450	15	60.5, 64.5		66.8	22	24	
450	20	69.8			22		
900		81.9−83.9[a]	99.3, 99.6	100	55	58	57

[a] Five measurements.

A chemical titration by sulfuric acid was used to determine the extent of nickel reduction following Coenen's method.[21] After reduction, the samples were cooled to 450 °C under argon (25 mL·min^{-1}) and maintained 1 h under hydrogen at this temperature. A given volume of sulfuric acid solution (9 N) was introduced under Ar into the reactor containing the reduced sample. According to the reaction, $Ni^0 + H_2SO_4 \rightarrow NiSO_4 + H_2$, the total dissolution of Ni^0 leads to hydrogen evolvment whose volume was measured thanks to a calibrated buret using the same type of equipment as described earlier by Coenen.[21] From the amount of Ni/SiO_2 sample and the volumes of acid added and hydrogen evolved, it is possible to calculate the amount of nickel metal and to deduce the average extent of nickel reduction. In view of the EPR spectra, the amount of Ni^I ions was considered to be negligible.[22]

Magnetic measurements (MM) of the reduced samples were also performed by the Weiss extraction method in order to determine the extent of reduction and also the average metal particle size. Details concerning the principle of the method can be found in refs 23−25. An electromagnet Varian 4012-3B providing fields up to 17 500 G was used. The measurements were performed at 77 K and room temperature. The samples were pressed (63×10^3 Pa·cm^{-2}) into wafers and transferred into the magnetic field in air-free conditions after reduction.

As it will be shown below, since the average size of metal particles and the nickel reducibility strongly depend on the reduction conditions, batches of 200 mg were systematically reduced before the experiments of TEM, H_2 chemisorption, chemical titration, and MM.

Results and Discussion

1. Comparison of the Measurements of the Extent of Ni Reduction and Metal Particle Size. The different methods, i.e., H_2 consumption during reduction, chemical titration by sulfuric acid, and MM, used to determine the extent of nickel reduction in the Ni/SiO_2 sample isothermally reduced at 450 °C for various times appear to be in good agreement (Table 1).

TABLE 2: Metal Particle Size Distribution in DP Ni/SiO_2 (24 wt % Ni) Reduced in Isotherm at 450 °C or by TPR Up to 900 °C under Standard Conditions. Comparison of the Results Obtained by TEM and MM

reduction temperature	450 °C (15 h)	450 °C (15 h)	900 °C	900 °C
technique	TEM	MM	TEM	MM
av particle diameter (Å)	22	24	55	57
particle size distribution	% particles[a]	% Ni[b]	% particles	% Ni
150 < *d* < 250 Å	0	0	0	4
25 < *d* < 150 Å	42	33	97	76
15 < *d* < 25 Å	28	28	3	17
d < 15 Å	30	39	0	3

[a] Percentage of particles obtained in each size range. [b] Percentage of Ni measured in each size range.

This is less satisfactory for the sample reduced by TPR up to 900 °C: the MM and chemical titration provide 100% of nickel reduction whereas the H_2 consumption indicates only ≈80% (Table 1). To understand this difference, Ni/SiO_2 was heated under standard TPR conditions except for the atmosphere, which was Ar here. An extent of 16% of nickel reduction was found by MM, indicating that a mere thermal treatment under an inert gas induces some nickel reduction. It is deduced that during TPR, a fraction of nickel is reduced between 450 and 900 °C without any H_2 consumption. This explains the lower percentage of reduction obtained from the H_2 consumption. This also indicates that the return to the baseline of the TPR trace is a good criterion for a full reduction of nickel.

The average nickel particle size in Ni/SiO_2 reduced by under standard TPR conditions or isothermally at 450 °C was measured by TEM, H_2 chemisorption, and MM. Table 1 shows a good agreement in the results. They also show that the particles in the sample reduced at 900 °C are larger than those in the sample reduced at 450 °C. The comparison of the particle size distributions obtained from TEM and MM (Table 2) shows that the numbers of particles below 15 and above 150 Å are underestimated by TEM. This is probably because (i) very small particles (<10 Å) cannot be observed by TEM and (ii) the largest particles are scarce, so the probability of finding them by TEM is low.

The XRD pattern of the sample isothermally reduced at 450 °C and exposed to air is characteristic of NiO whereas that of the sample reduced by TPR up to 900 °C is characteristic of Ni^0. These results indicate that when they are exposed to air, the small metal particles (≈20 Å) formed at 450 °C are more easily and deeply oxidized than the larger ones (≈60 Å) obtained at 900 °C. In previous studies on the passivation of nickel metal particles supported on silica, the depth of the passivated layer was estimated to be two monolayers by Coenen and Linsen[26] on the basis of quantitative X-ray analysis, three monolayers by Dell et al.[27] on the basis of oxygen chemisorption measurements, and three−four monolayers by Montes et al.[9] on the basis of combined electron microscopy and XPS analyses. From these studies, one can estimate that the particles smaller than 25 Å are almost totally oxidized, which explains why NiO is detected by XRD in the sample isothermally reduced at 450 °C.

2. Mechanism of Reduction of Ni/SiO_2 Samples (According to the Literature). It has been shown in our previous paper[3] that the mechanism of reduction of silica-supported $Ni(OH)_2$ proposed by Martin et al.[28] and reported in Figure 2 could explain the different average sizes of metal particles obtained on various DP Ni/SiO_2 samples reduced by TPR under standard conditions. We also checked that (i) reduction takes place once the Ni(II) precursor is decomposed (step 1); (ii) the higher the decomposition temperature of the Ni(II) precursor, the more efficiently water is eliminated from the sample before reduction, and the smaller the metal particles. This means that when water is efficiently eliminated, reduction of nickel via step 3 is favored over reduction via steps 2 and 4, and conversely, sintering of the oxide phase via step 2 is prevented. We also showed that sintering of Ni^0 (step 5) is not important between 650 and 900 °C.

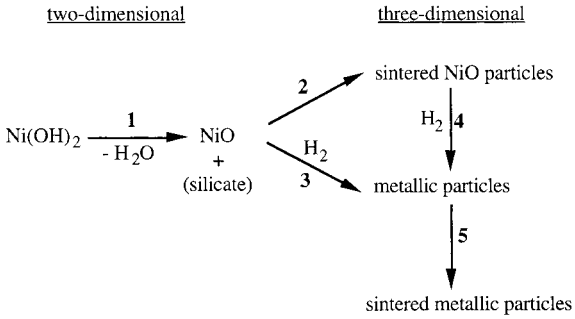

Figure 2. Mechanism of reduction of silica-supported nickel samples from ref 28.

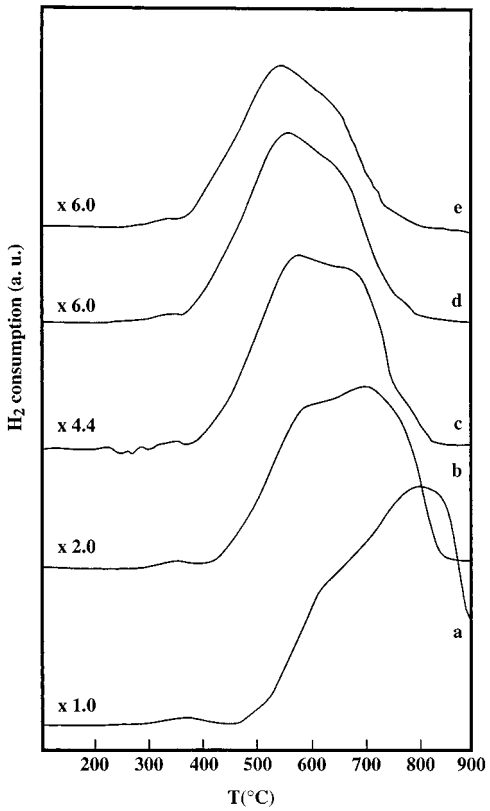

Figure 3. TPR profiles of DP Ni/SiO_2 (24 wt % Ni) obtained with the constant heating rate of 7.5 °C·min^{-1} and various H_2/Ar flow rates: (a) 10; (b) 25; (c) 50; (d) 75; (e) 100 mL·min^{-1}.

In the following, we will examine if this mechanism of reduction remains consistent with the different conditions of reduction.

3. Influence of the Conditions of Reduction by TPR on the Metal Particle Size. *a. Standard Conditions.* The TPR profile of the sample reduced in standard conditions is reported in Figures 3b and 5d. It exhibits a broad asymmetric peak with a maximum at ≈700 °C and a shoulder at ≈600 °C, arising from the reduction of supported 1:1 nickel phyllosilicate.[1] The metal particles measured from electron micrographs have an average size of ≈55 Å (Tables 1 and 3, sample 1) and a size distribution between 20 and 100 Å (Figures 4b and 5c).

TABLE 3: Influence of the TPR Parameters on the Average Metal Particle Size in DP Ni/SiO_2 (24 wt % Ni). Comparison of the Results Obtained by H_2 Chemisorption and TEM

	reduction conditions			av metal particle dia (Å)	
sample	final temp (°C)	H_2/Ar flow rate (mL·min^{-1})	heating rate (°C·min^{-1})	H_2 chemisorpn	TEM
1	900	25	7.5	58	55
2[a]	900	10	7.5		78
1	900	25	7.5	58	55
3	900	50	7.5	45	42
4	900	75	7.5	39	36
5	900	100	7.5	38	34
6	900	25	15.0	65	64
1	900	25	7.5	58	55
7	900	25	5.0	52	
8	900	25	2.5	40	38
9	900	25	1.0	44	41
10	800	100	7.5	34	30
11	800	25	2.5	44	
12	800	100	2.5	36	
13	900/1 h	25	15.0	64	64
14[b]	900	25	15.0	71	

[a] Partially reduced nickel. [b] Calcined at 800 °C for 1 h before TPR.

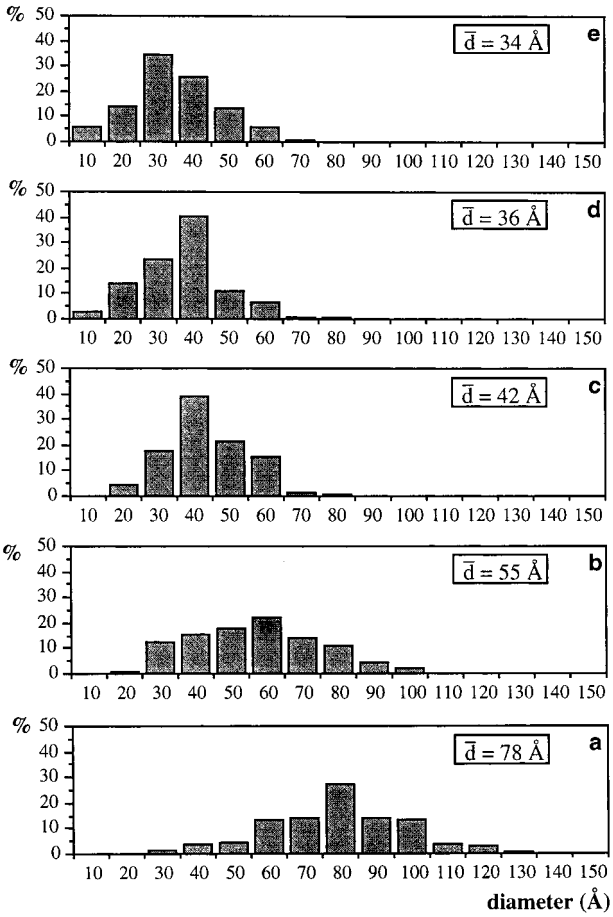

Figure 4. Histograms of metal particle diameters and average diameters of DP Ni/SiO_2 (24 wt % Ni) reduced by TPR up to 900 °C with the constant heating rate of 7.5 °C·min^{-1} and various H_2/Ar flow rates: (a) 10; (b) 25; (c) 50; (d) 75; (e) 100 mL·min^{-1}.

b. Influence of the H_2/Ar Gas Flow Rate. The TPR profiles obtained for various H_2/Ar gas flow rates from 10 to 100 mL·min^{-1} and the heating rate of 7.5 °C min^{-1} are reported in Figure 3. While the TPR peak shifts toward lower temperatures when the gas flow rate increases, its shape does not change much. It can be noted that the gas flow rate of 10 mL·min^{-1} does not lead to total reduction at 900 °C since there is no return of the TPR trace to the baseline. Hence, the increase in the H_2/

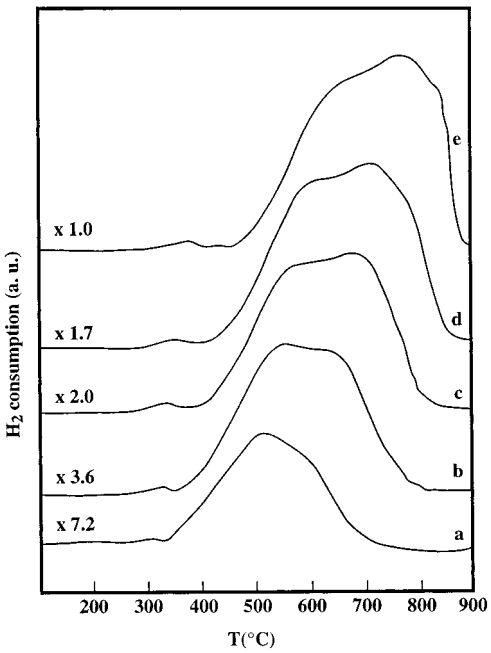

Figure 5. TPR profiles of DP Ni/SiO_2 (24 wt % Ni) obtained with the constant H_2/Ar flow rate of 25 mL·min^{-1} and various heating rates: (a) 1.0; (b) 2.5; (c) 5; (d) 7.5; (e) 15 °C·min^{-1}.

Ar flow rate from 10 to 100 mL·min^{-1} lowers the reduction temperature of Ni(II) (Figure 3). In addition, it leads to smaller metal particles from 78 to 34−38 Å (samples 1−5 in Table 3) and a narrowing of the size distribution (Figure 4).

These results are consistent with the mechanism of reduction reported in Figure 2. Indeed, the increase of the reducing gas flow rate leads to a more efficient elimination of the water originally present in the sample and also produced during reduction. As a consequence, the dehydration of the Ni(II) phase is favored, and the reduction as well, and NiO sintering (step 2) is inhibited. Therefore, smaller metal particles are obtained.

It may be noted that flow rates higher than 75 mL·min^{-1} have no effect on the particle size (Figure 4), i.e., no effect on the kinetics of dehydration of the Ni(II) phase and of its subsequent reduction.

c. Influence of the Heating Rate. When the heating rate decreases from 15 to 1 °C·min^{-1}, and for the flow rate of 25 mL·min^{-1}, the TPR peaks shift toward lower temperatures (Figure 5), as does the final reduction temperature. Meanwhile the size distribution of the metal particles becomes narrower (Figure 6), and the average size decreases from 64−65 Å to 38−40 Å (samples 1 and 6−9 in Table 3) before slightly increasing again to 41−44 Å for the heating rate of 1 °C·min^{-1}.

These results are also consistent with the mechanism of reduction (Figure 2): when the heating rate decreases, the thermal decomposition of the Ni(II) phase is slower but water is eliminated more efficiently. So, step 3 of reduction is favored over steps 2 and 4, reduction proceeds at a lower temperature, and the particles are smaller. However, the metal particles are larger for the heating rate of 1 °C·min^{-1} (44 Å) compared to 2.5 °C·min^{-1} (40 Å). This may indicate that slight metal sintering occurs between the end of nickel reduction at ≈750 °C and the end of the TPR at 900 °C, i.e., during the 2.5 h of the 1 °C·min^{-1} heating ramp.

The TPR profile of sample 5 (100 mL·min^{-1} and 7.5 °C·min^{-1}) (Figure 3e) is the same as that obtained by Keane[14] for two DP Ni/SiO_2 samples (200 mg, 12 and 20 wt % Ni) reduced under 6% v/v H_2 in N_2 with a higher flow rate (150

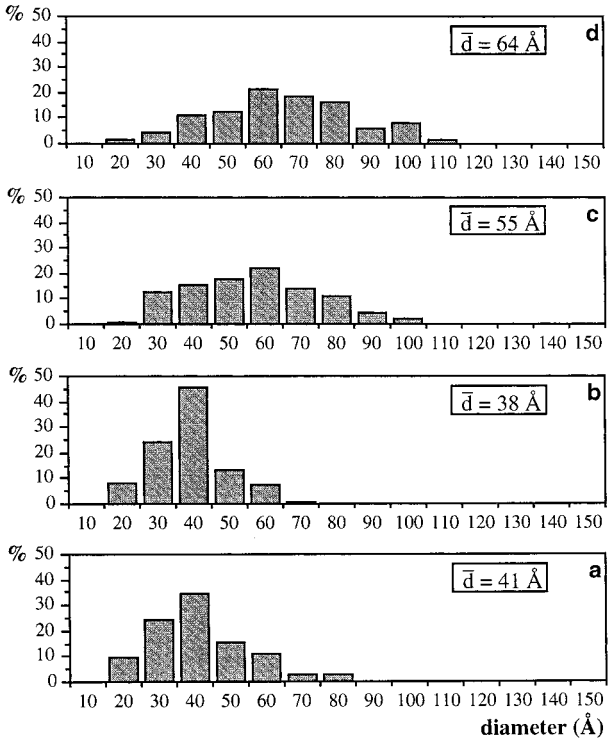

Figure 6. Histograms of metal particle diameters and average diameters of DP Ni/SiO_2 (24 wt % Ni) reduced by TPR up to 900 °C with the constant H_2/Ar flow rate of 25 mL·min^{-1} and various heating rates: (a) 1.0; (b) 2.5; (c) 5; (d) 7.5; (e) 15 °C·min^{-1}.

mL·min^{-1}) and a lower heating rate (5 °C·min^{-1}) than those used in the present work: the TPR profiles exhibit the same temperature maximum (540−580 °C). These results are also consistent with the mechanism of reduction; i.e., a higher flow rate increases the reduction temperature while a lower heating rate lowers it.

d. Influence of the Final TPR Temperature. It can be shown in Figures 3e and 5a that the TPR traces return to the baseline before 800 °C when the gas flow rate is high (100 mL·min^{-1}) or the heating rate is low (≤2.5 °C·min^{-1}). So, we have also tried to form metal particles smaller than 34−38 Å (sample 5) in lowering the final temperature of reduction to 800 °C.

Hence, for the high gas flow rate of 100 mL·min^{-1} and the heating rate of 7.5 °C·min^{-1}, the average metal particle size is slightly smaller (30−34 Å for sample 10 in Table 3) when TPR is stopped at 800 °C rather than at 900 °C (34−38 Å for sample 5). In contrast, for the low H_2/Ar flow rate of 25 mL·min^{-1} and the heating rate of 2.5 °C·min^{-1}, the average size is larger than expected: 44 Å at 800 °C (sample 11) instead of 38−40 Å at 900 °C (sample 8). Finally, the combination of a high gas flow rate (100 mL·min^{-1}) and of a low heating rate (2.5 °C·min^{-1}) does not lead to significantly smaller particles at 800 °C since an average size of 36 Å is obtained (sample 12).

These results will be discussed in section 5.b.

4. Isothermal Reduction at 450 °C. The above results indicate that it is not possible to lower the average metal particle size below 30−34 Å (sample 10) when nickel is fully reduced.

This has prompted us to perform isothermal reduction at 450 °C. However, the reduction of nickel was incomplete. Indeed, between 5 and 20 h of reduction at 450 °C, the extent of nickel reduction increases between 35 and 70% (Table 1), but it remains below 100%. The profile of H_2 consumption is given in Figure 7. The average metal particle size is ≈22 Å whether

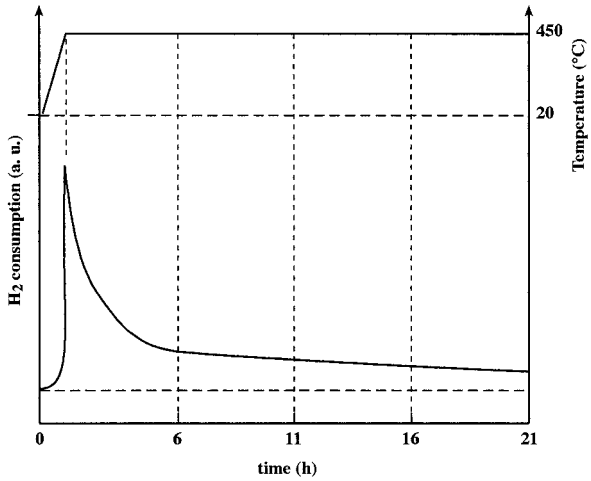

Figure 7. H_2 consumption profile during isothermal reduction at 450 °C of DP Ni/SiO_2 (24 wt % Ni) under the H_2/Ar flow rate of 25 mL·min^{-1}.

it is measured by H_2 chemisorption or TEM and does not seem to depend on the reduction time or the particle size distribution (10−60 Å).

These results are in agreement with other studies on the effect of the reduction time at 400−500 °C on the particle size and the extent of reduction in DP Ni/SiO_2 samples.[6,19] They are also consistent with the fact that (i) after reduction at 450 °C, the electron micrographs show both layered structures of nickel phyllosilicates and metal particles (Figure 8); (ii) it is necessary to reach 600 °C to obtain the complete decomposition of supported nickel phyllosilicate into NiO and SiO_2;[3] (iii) decomposition precedes reduction (Figure 2).

The average particle size is smaller (≈20 Å) than when nickel is fully reduced by TPR up to 900 °C (Table 3). Coenen [19] obtained similar results on EuroNi-1 (Ni/SiO_2 prepared by DP with 25 wt % Ni): after reduction at 450 °C for 4 h, the average particle size was ≈23 Å and nickel was partially reduced. He also showed that after reduction at 650 °C for 3 h the average particle size was ≈45 Å and nickel was fully reduced.

5. Sintering. We have also tried to get samples with particles larger than 65 Å.

a. Sintering of Nickel Oxide Particles. The first attempt was to sinter first the supported Ni(II) phase before running standard TPR (sample 14). The fresh sample was calcined for 1 h under oxygen with the flow rate of 25 mL·min^{-1} at 800 °C. After TPR, the results obtained by H_2 chemisorption show that the metal particles are slightly larger (71 Å) than in sample 1 directly reduced (58 Å) (Table 3).

According to Martin et al.,[28] NiO particles are reduced into Ni^0 through step 4 without mass transfer of nickel, i.e., without nickel migration onto the silica surface during reduction. One can deduce that the slightly larger average size of metal particles arises from a low extent of NiO sintering during calcination. No significant sintering was observed by Richardson and Dubus [6] and Keane[14] when DP Ni/SiO_2 samples were calcined before reduction. This could be explained by the fact that their calcination temperatures were lower (350−500 °C) than the temperature of decomposition of nickel phyllosilicates (600 °C, as mentioned in section 4). However, in the present work, the calcination temperature (800 °C) is high enough to decompose the phyllosilicates, but sintering of NiO is not significant either.

Sintering of NiO is much more moderate than that in impregnated Ni/SiO_2 samples (6.1 wt % Ni, the same silica as here, nickel nitrate precursor): aggregates of 300−800 Å in

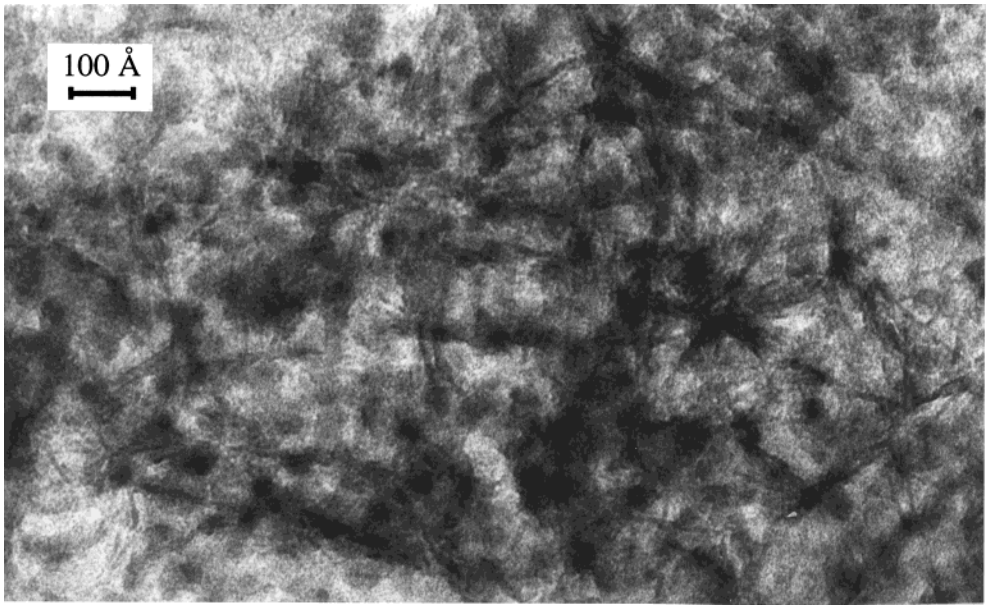

Figure 8. Electron micrograph of DP Ni/SiO_2 (24 wt % Ni) reduced at 450 °C for 10 h.

diameter consisting of nickel metal particles of 100−200 Å after calcination at 600 °C for 2 h and TPR up to 700 °C[29] instead of an average particle size of 68 Å after direct TPR up to 700 °C. The different resistance to NiO sintering in these two types of samples is probably due to the different temperatures of decomposition of the supported Ni(II) phases: 600 °C for nickel phyllosilicate and ≈300 °C for nickel nitrate.[29] Hence, less water is present in the DP Ni/SiO_2 samples when decomposition occurs to induce NiO sintering (step 2 in Figure 2).

b. Sintering of Ni^0 Particles. The second attempt was to sinter the metal particles after reduction by TPR up to 900 °C. Hence, the sample was maintained for 1 h at 900 °C under H_2/Ar, but the particle size remained unchanged (compare samples 6 and 13 in Table 3). No Ni^0 sintering was observed either during the TPR between 800 and 900 °C with the heating rate of 2.5 °C·min^{-1}, i.e., during the 40 min of heating between 800 and 900 °C: 44 Å at 800 °C and 40 Å at 900 °C (samples 11 and 8 in Table 3) (see section 3.d).

Hence, it has not been possible to obtain metal particles larger than 65 Å in this sample in varying the reduction conditions. This point is not consistent with the mechanism of reduction proposed by Martin, which reports a step of Ni^0 sintering (step 5 in Figure 2) when reduction is performed at high temperature (>600 °C) and during a long time. Coenen[19] reported that an increase in the time of reduction at 650 °C up to 45 h does not induce either any significant increase in the size of metal particles in DP Ni/SiO_2 samples. The high resistance to sintering of nickel metal particles in DP Ni/SiO_2 samples was also observed during cyclic treatments in H_2 at 500 °C or O_2 at 450 °C,[10] during stability tests of calcination with or without previous reduction under H_2[13] and during reactions of benzene hydrogenation [9] and CO hydrogenation.[30]

c. Resistance to Sintering. According to the literature,[9,10,14] the resistance to metal sintering of samples prepared by DP would be due to strong metal−support interaction. However, little is known concerning the nature of this interaction.

Delmon et al.[9,12] proposed that the particles are partially embedded in the support after reduction, the silica remnants acting as spacers of the particles and stabilizing the particles against sintering. However, this interpretation does not fit our experimental results. Indeed, there is a good agreement between the measurement of the average particle size by TEM, H_2 chemisorption, and MM, which indicates that the whole surface of the metal particles is accessible to H_2 (Table 1) and therefore that the metal particles are not embedded in silica.

Praliaud and Martin[31] found evidence for the formation of strong metal−support interaction in Ni/SiO_2 samples prepared by "reacting silica with nickel nitrate hexaammine", then reduction at low heating rate (2 °C·min^{-1}) up to 850 °C. Their magnetic measurements showed that the specific saturation magnetization measured at 25 °C drops to zero when the reduction temperature is 850 °C, indicating a loss of the ferromagnetic properties of metal nickel. To explain this result, they proposed the formation of nickel silicide. This interpretation was confirmed by Lamber et al.[32] in Ni/SiO_2 samples prepared by vacuum evaporation of nickel on thin films of SiO_2. They observed the formation of Ni_3Si intermetallic compound after heating at 480 °C for 100 h under hydrogen. Electron diffraction analysis showed that a fraction of the smaller Ni cristallites (≤50 Å) was fully transformed into Ni_3Si while larger particles (>100 Å) were often composed of Ni metal and Ni_3Si. More recently, the same team also detected[33] the presence of nickel silicide in Ni/SiO_2 samples prepared by sol−gel and reduced in hydrogen at 650 °C for 10 h. In all these studies, the conditions of formation of nickel silicide are close to the conditions of reduction of our DP Ni/SiO_2 sample by TPR. We did not perform experiments of electron diffraction with our reduced samples. However, the measurements of the extents of reduction and of the average particle sizes by magnetic method (Tables 1 and 2) are fully consistent with those obtained by the other methods, so nickel silicide does not seem to form significantly in our sample.

Other types of metal−support interaction are proposed in the literature. According to Dalmai-Imelik et al.,[34] bulk 1:1 nickel phyllosilicate leads to hexagonal platelets of nickel crystallites with either (111) or (110) planes parallel to the silica sheets depending on the conditions of reduction at 700 °C. Coenen[19] suggested that the metal crystallites are attached epitaxially to silica through a monolayer of Ni^{2+} ions arising from nickel phyllosilicate, which induces a strong bonding layer. Several experimental[35−38] and theoretical[39] studies also suggested that after reduction, unreduced ions remain at the metal−support interface. We therefore propose that the interface between the nickel metal particles and silica still contains ionic nickel species

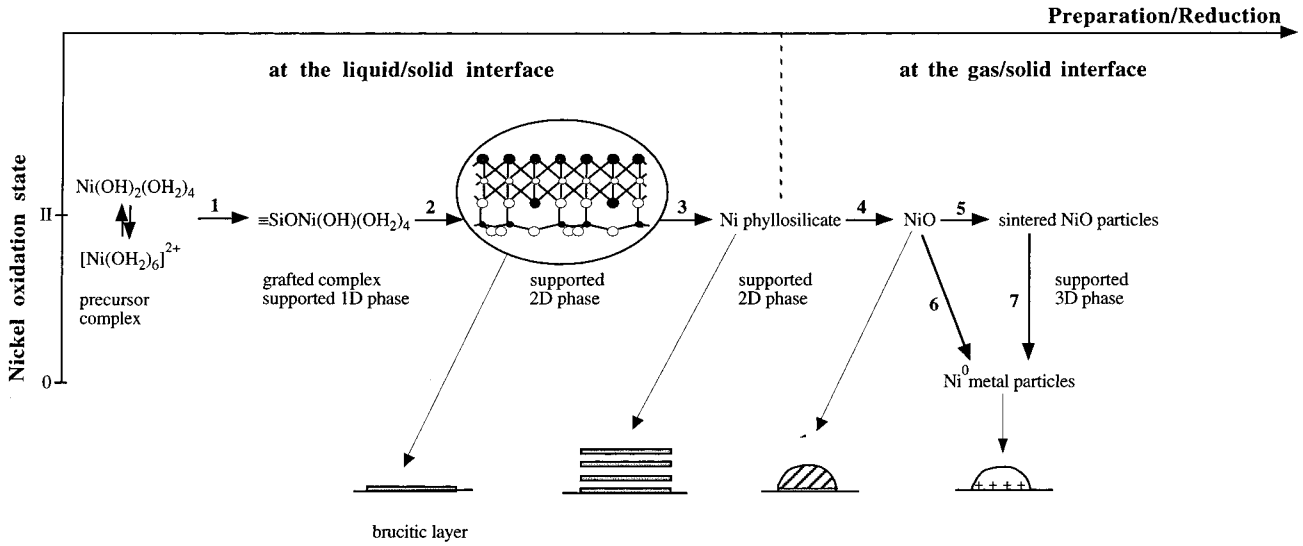

Figure 9. Genesis of the formation of small metal particles, highly resistant to sintering, for the Ni/SiO_2 sample prepared by deposition−precipitation.

but in too low a concentration to be detected by TPR. They would arise from the decomposition of nickel phyllosilicate at the Ni(II)−support interface. These ions bonded to the silica surface would act as grafting sites for the metal particles, leading to their stabilization and favoring the metal dispersion and the resistance to sintering.

6. Mechanism of Formation of Metal Particles. As mentioned in the Introduction, this paper is the last one of a series of four devoted to the preparation and the characterization of DP Ni/SiO_2 samples.[1−3] What is important in the preparation by DP is the formation of supported nickel phyllosilicate. The reduction leads to the formation of metal particles with diameters smaller than 100 Å. This size cannot vary within a large range owing to the high resistance of both NiO and Ni^0 to sintering. All these results may be integrated into a general scheme (Figure 9), starting from the very beginning of the preparation in solution, i.e., when the $[Ni(OH_2)_6]^{2+}$ complex in equilibrium with $[Ni(OH)(OH_2)_5]^+$ and $Ni(OH)_2(OH_2)_4$ is in electrostatic interaction with the silica support. The Ni(II) hydroxoaqua complexes close to the silica surface can react with the silanol groups via an hydrolytic adsorption (step 1). They can also react with each other via olation reaction to form a brucitic layer of octahedral Ni(II) bonded to the silica surface (step 2). It may be noted that this brucitic layer bonded to silica can also be considered as a sheet of 1:1 nickel phyllosilicate (Figure 1) at the support−solution interface. Meanwhile, silica dissolves and the silicic acid released in solution can react with the nickel complexes in solution via an heterocondensation reaction to form Si−O−Ni monomers that polymerize and grow on the brucitic layer of Ni(II) bonded to silica, so as lead to supported 1:1 nickel phyllosilicate (step 3). During the washing and drying steps after DP, the supported phase remains the same. Then, the sample is reduced. Reduction goes through a step of decomposition of the supported phase into NiO and SiO_2 (step 4). The NiO phase hardly sinters (step 5), most probably because of the strong metal oxide−support interaction due to the presence of a brucitic layer at the interface. Step 5 explains that slightly different metal particle sizes are obtained when the heating rate and the flow rate vary (Table 3). Then, NiO particles are reduced (steps 6 or 7), and Ni^0 hardly sinters most probably because of the strong metal−support interaction due to the presence of unreduced Ni ions at the interface that would act as grafting sites for the metal particles.

Conclusion

This paper deals with the reduction of a Ni/SiO_2 sample (24 wt % Ni) prepared by deposition−precipitation whose supported Ni(II) phase is a 1:1 nickel phyllosilicate.[1] TPR up to 900 °C leads to the full reduction of nickel with an average metal particle size (35−65 Å) that depends on the following parameters: heating rate, H_2/Ar flow rate, and final temperature, 800 or 900 °C (Table 3). Slow heating rate and high H_2/Ar flow rate favor the formation of small metal particles.

It is possible to prepare smaller metal particles of ≈20 Å by isothermal reduction at 450 °C (Table 1), but nickel is not fully reduced. This temperature is too low to lead to the full decomposition of the nickel phyllosilicate before its reduction.

Because of the high resistance to sintering of the nickel oxide particles before reduction and of the metal particles during reduction, the average metal particle size cannot exceed 70 Å. The high resistance to sintering is explained by the strong metal oxide− and metal−support interaction.

To conclude our series of papers devoted to the preparation and characterization of Ni/SiO_2 catalysts prepared by deposition−precipitation,[1−3] it may be claimed that the formation of supported nickel phyllosilicate is a request to obtain after reduction small metal particles highly resistant to sintering. The metal particles are located on the support surface since they chemisorb hydrogen. A general scheme summarizing the whole genesis of these particles from the very beginning of the Ni/SiO_2 preparation is proposed in Figure 9.

Acknowledgment. The authors are indebted to Rhône Poulenc (France) for financial contribution of this work.

References and Notes

(1) Burattin, P.; Che, M.; Louis, C. *J. Phys. Chem. B* **1997**, *101*, 7060.
(2) Burattin, P.; Che, M.; Louis, C. *J. Phys. Chem. B* **1998**, *102*, 2722.
(3) Burattin, P.; Che, M.; Louis, C. *J. Phys. Chem. B* **1999**, *103*, 6171.
(4) Nickel hydroxide with a turbostratic structure: bidimensional structure because of the disordered stacking of the brucitic layers of octahedral Ni(II), α-$Ni(OH)_2$.
(5) 1:1 nickel phyllosilicate: layered compound of structural formula $Si_2Ni_3O_5(OH)_4$, also called serpentine, or Ni-lizardite or nepouite when the layers are planar, Ni-antigorite when the layers are splintery, or Ni-chrysotile when they are curled into cylindrical rolls. A layer of 1:1 nickel phyllosilicate consists of a brucite-type sheet containing Ni(II) in octahedral coordination and a sheet containing linked tetrahedral SiO_4 units.
(6) Richardson, J. T.; Dubus, R. J. *J. Catal.* **1978**, *54*, 207.

(7) Richardson, J. T.; Dubus, R. J.; Crump, J. G.; Desai, P.; Osterwalder, U.; Cale, T. S. *Stud. Surf. Sci. Catal.* **1979**, *3*, 131.
(8) Coenen, J. W. E. *Stud. Surf. Sci. Catal.* **1979**, *3*, 89.
(9) Montes, M.; Penneman de Bosscheyde, C.; Hodnett, B. K.; Delannay, F.; Grange, P.; Delmon, B. *Appl. Catal.* **1984**, *12*, 309.
(10) Montes, M.; Soupart, J. B.; de Saedeleer, M.; Hodnett, B. K.; Delmon, B. *J. Chem. Soc., Faraday Trans. 1* **1984**, *80*, 3209.
(11) Blackmond, D. A.; Ko, E. I. *Appl. Catal.* **1984**, *13*, 49.
(12) Delmon, B. *J. Mol. Catal.* **1990**, *59*, 179.
(13) Gil, A.; Diaz, A.; Gandia, L. M.; Montes, M. *Appl. Catal., A* **1994**, *109*, 167.
(14) Keane, M. A. *Can. J. Chem.* **1994**, *72*, 372.
(15) Keane, M. A.; Patterson, P. M. *J. Chem. Soc., Faraday Trans.* **1996**, *92*, 1413.
(16) van Eijk van Voorthuijsen, J. J. B.; Franzen, P. *Rec. Trav. Chim. Pays Bas* **1951**, *70*, 793.
(17) Martin, G. A.; Renouprez, A.; Dalmai-Imelik, G.; Imelik, B. *J. Chim. Phys.* **1970**, *67*, 1149.
(18) Mallet, P.; Cabarello, A. *J. Chem. Soc., Faraday Trans. 1* **1988**, *84*, 2369.
(19) Coenen, J. W. E. *Appl. Catal.* **1991**, *75*, 193.
(20) Burattin, P. Ph.D. Thesis, Université Pierre et Marie Curie, Paris, 1994.
(21) Coenen, J. W. E. *Appl. Catal.* **1989**, *54*, 65.
(22) Bonneviot, L.; Cai, F. X.; Che, M.; Kermarec, M.; Legendre, O.; Lepetit, C.; Olivier, D. *J. Phys. Chem.* **1987**, *91*, 5912.
(23) Weiss, P.; Forrer, R. *Ann. Phys.* **1926**, *5*, 153.
(24) Primet, M.; Dalmon, J. A.; Martin, G. A. *J. Catal.* **1977**, *46*, 25.
(25) Guilleux, M. F.; Delafosse, D.; Martin, G. A.; Dalmon, J. A. *J. Chem. Soc., Faraday Trans. 1* **1979**, *75*, 165.
(26) Coenen, J. W. E.; Linsen, B. G. In *Physical and Chemical Aspects of Adsorbents and Catalysts*; B. G. Linsen, Ed.; Academic Press: London, 1970; p 471.
(27) Dell, R. M.; Klemperer, D. F.; Stone, F. S. *J. Phys. Chem.* **1956**, *60*, 1586.
(28) Martin, G. A.; Mirodatos, C.; Praliaud, H. *Appl. Catal.* **1981**, *1*, 367.
(29) Louis, C.; Cheng, Z. X.; Che, M. *J. Phys. Chem.* **1993**, *97*, 5703.
(30) Martra, G. M.; Swaan, H. M.; Mirodatos, C.; Kermarec, M.; Louis, C. *Stud. Surf. Sci. Catal.* **1997**, *111*, 617.
(31) Praliaud, H.; Martin, G. A. *J. Catal.* **1981**, *72*, 394.
(32) Lamber, R.; Jaeger, N.; Schultz-Ekloff, G. *Surf. Sci.* **1990**, *227*, 268.
(33) Ueckert, T.; Lamber, R.; Jaeger, N. I.; Shubert, U. *Appl. Catal.* **1997**, *155*, 75.
(34) Dalmai-Imelik, G.; Leclercq, C.; Maubert-Muguet, A. *J. Solid State Chem.* **1976**, *16*, 129.
(35) Huizinga, T.; Prins, R. *J. Phys. Chem.* **1983**, *87*, 173.
(36) Turlier, P.; Praliaud, H.; Moral, P.; Martin, G. A.; Dalmon, J. A. *Appl. Catal.* **1985**, *19*, 287.
(37) Bonneviot, L.; Che, M.; Olivier, D.; Martin, G. A.; Freund, E. J. *J. Phys. Chem.* **1986**, *90*, 2112.
(38) Haberlandt, H.; Ritschl, F. *J. Phys. Chem.* **1986**, *90*, 4322.
(39) Che, M.; Masure, D.; Chaquin, P. *J. Phys. Chem.* **1993**, *97*, 9022.